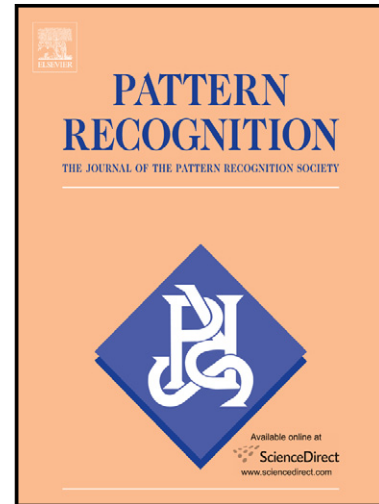


Author's Accepted Manuscript

Ecds: An Effective Shape Signature using
Electrical Charge Distribution on the Shape

Zhiyang Li, Wenyu Qu, Junjie Cao, Heng Qi,
Keqiu Li, Milos Stojmenovic



PII: S0031-3203(14)00323-9
DOI: <http://dx.doi.org/10.1016/j.patcog.2014.08.009>
Reference: PR5192

To appear in: *Pattern Recognition*

Received date: 15 January 2014
Revised date: 5 June 2014
Accepted date: 13 August 2014

Cite this article as: Zhiyang Li, Wenyu Qu, Junjie Cao, Heng Qi, Keqiu Li, Milos Stojmenovic, Ecds: An Effective Shape Signature using Electrical Charge Distribution on the Shape, *Pattern Recognition*, <http://dx.doi.org/10.1016/j.patcog.2014.08.009>

This is a PDF file of an unedited manuscript that has been accepted for publication. As a service to our customers we are providing this early version of the manuscript. The manuscript will undergo copyediting, typesetting, and review of the resulting galley proof before it is published in its final citable form. Please note that during the production process errors may be discovered which could affect the content, and all legal disclaimers that apply to the journal pertain.

ECDS: An Effective Shape Signature using Electrical Charge Distribution on the Shape

Zhiyang Li, College of Information Science and Technology, Dalian Maritime University,
116026, China

Wenyu Qu, College of Information Science and Technology, Dalian Maritime University,
116026, China

Junjie Cao, School of Mathematical Sciences, Dalian University of Technology, 116023,
China

Heng Qi, School of Computer Science and Technology, Dalian University of Technology,
116023, China

Keqiu Li, School of Computer Science and Technology, Dalian University of Technology,
116023, China

Milos Stojmenovic, Department of Informatics and Computing, Singidunum University,
Belgrade, Serbia

Corresponding author: Wenyu Qu, TEL.: +86-411-84723505, FAX: +86-411-84723505,
Email: wenyu@dlnu.edu.cn, Address: No.1 Linghai Road, Dalian, China, 116026.

ECDS: An Effective Shape Signature using Electrical Charge Distribution on the Shape

Zhiyang Li¹, Wenyu Qu^{1,*}, Junjie Cao², Heng Qi³, Keqiu Li³, Milos Stojmenovic⁴

Abstract

Motivated by the fact that electrical charge distributions are almost the same for similar shapes but not vice versa when shapes reach their electrical equilibrium condition, we propose a novel shape signature based on the electrical charge distribution on the shape (ECDS). Compared to other shape signatures, ECDS has the following interesting properties: 1) ECDS is a local measure but computed in a global manner. Thus, it is more robust to noise and shape variations. 2) ECDS is articulation insensitive and therefore exhibits better performance by the introduction of generalized coulomb potentials. This allows it to better match shapes whose parts can move independently, such as scissors. 3) The sum of ECDS remains constant during the process of reaching electrical equilibrium, which does favor some applications. Numerous experiments have been done on several public shape databases (MPEG-7 database, articulated shape data set, Kimia silhouettes and ETH-80 data set), demonstrating that ECDS has the above properties and compares well with other shape descriptors in many kinds of shape retrieval and recognition tasks.

Keywords:

Shape representation, shape matching, generalized electrical potential, electrical charge distribution.

*wenyu@dlnu.edu.cn

¹College of Information Science and Technology, Dalian Maritime University, China

²School of Mathematical Sciences, Dalian University of Technology, China

³School of Computer Science and Technology, Dalian University of Technology, China

⁴Department of Informatics and Computing, Singidunum University, Belgrade, Serbia

1. Introduction

Due to the rapid development of imaging technologies and the internet, it is convenient for people to reference and obtain a large number of images, and applications such as image retrieval and recognition have become very common. However, textual annotation of images is inefficient and sometimes impossible in large image database. Retrieval by image content (CBIR) may be used instead of textual annotation [1]. The shape, as the most important feature of an image, plays a prominent role in the content-based search method. Compared to color or texture, shape alone can represent the whole object, but common shapes require hundreds of parameters to be represented explicitly [2]. In order to more easily handle, store and compare shapes, researchers propose to represent shapes by intelligent descriptors using simplified representations that carry most of the important information. Thus, finding meaningful and efficient shape descriptors is a fundamental problem in shape retrieval and recognition.

Since the contour or silhouette is the most important feature of a shape, various shape descriptors based on the contour are proposed in the literature. Early contour-based descriptors consider the contour as a whole and represent it by some global measures such as area, eccentricity, chord context, invariant moments, spectral coefficients and so on [3, 4, 5, 6, 7]. In general, global descriptors are compact and efficient for comparison. However, most of these descriptors have only low discrimination and are sensitive to large deformations of the shape. An example is shown in the first pair of shapes in Fig. 1. Since local geometry information is lost in global descriptors, it is not easy for global descriptors to capture the part similarity between the camels. Thus, recently proposed shape descriptors focus on local features and hybrid (global/local) descriptors. The shape signature is an important example of these kinds of descriptors.

Shape signature is usually defined as any 1-D function on a shape, derived from the shape contour points. Compared to other shape descriptors such as shape context or multi-scale shape descriptors, shape signatures can capture the essential information of the shape in a more compact manner. Early proposed signatures include centroid distance, complex coordinates, curvature, tangent angle, local diameters, etc. [3, 4, 8]. They are concise and compact representations of the shapes and widely used in many shape analysis and recognition tasks. But most of these shape signatures fail to discriminate shapes with large differences. Recently, Xu et al. [9] propose a novel shape

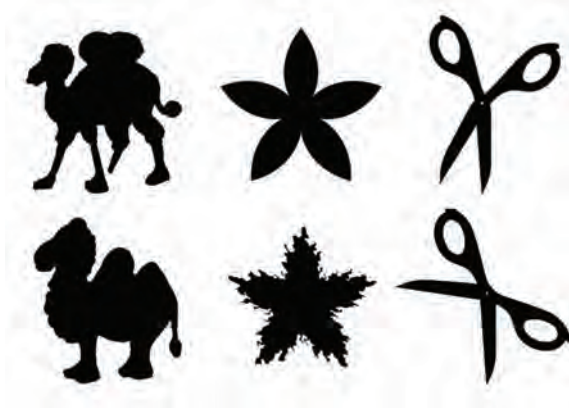


Figure 1: Three pairs of shapes that may be mismatched by existing methods.

signature called contour flexibility, which represents the deformable potential at each landmarks of the contour. The retrieval experiments in the MPEG7 shape database show that contour flexibility obtains the highest Bullseye scores among the shape signatures. However, although many kinds of shape signatures have been presented in the literature, the existing signatures have the following problems:

- Nearly all the shape signatures are estimated from the neighbors of each point, such as curvature, tangent angle, contour flexibility. Neighbor size is reported to usually have a significant impact on the signatures, especially when substantial noise is present. Noise is therefore widespread in the shape data (the second pair of shapes in Fig. 1). Introducing multi-scale or scale space techniques [10] can reduce this sensitivity but are computationally demanding for the shape matching process.
- Most shape signatures are not invariant to articulation (isometric transformation of the shape), since they are computed in a local way. As a result, the third pair of shapes in Fig. 1 may cause mismatching by these signatures, because articulation between two shapes introduces adverse information to the signatures. Effective shape signatures should capture both the local geometry information and part structure of the shape in a hybrid manner.
- In general, the existing signatures cannot yet provide entirely satis-

factory solutions to describe the shape variations well and have low performance in shape retrieval and recognition experiments, since they are only 1-D functions on the shape. A natural improvement is utilizing N-D functions, such as shape context [11, 12]. However, shape context is less compact and computationally demanding, like other multi-scale methods.

Based on the above observation, it is useful to propose a shape signature which can overcome the mentioned problems and perform as well as or even better than state-of-the-art shape descriptors. Aiming at this goal, we propose an effective shape signature named ECDS. Supposing that a 2D shape is a charged conductor, the basic idea of ECDS is representing the shape by its electrical charge distribution when the shape reaches the state of electrostatic equilibrium. Since charge tends to accumulate at a sharp convexity and vanish at a sharp concavity [13], the proposed ECDS descriptor captures the local curvature information and part structure of the shape. Meanwhile, ECDS is computed as the solution of a system of linear equations, which considers all data points at once. It makes ECDS more resilient to noise than other signatures, such as curvature.

The contributions are summarized as follows:

- A novel shape signature ECDS, which is invariant to translation, scale, rotation and insensitive to noise and articulation, is proposed.
- Different from the classic electrical charge distribution, ECDS is computed based on the generalized coulomb potential representing part-aware metric and long-range interactions, which significantly increases its descriptive power.
- Numerous experiments have been done on several public shape databases demonstrating that ECDS performs as well as or even better than the state-of-the-art shape descriptors, including the shape signatures, the shape context and the multi-scale descriptors.

The rest of this paper is organized as follows: Section 2 gives a brief overview of related work on shape representation methods. Section 3 presents ECDS representation and its computation. The generalized electrical potential and the characteristics of ECDS are also discussed in this section. Section 4 contains the description of the implementation and some experimental results. Finally, Section 5 summarizes the paper.

2. Related Work

As a hot topic in computer vision, shape representation and analysis has been extensively studied. Since shapes commonly are 2D images which are projections from 3D objects, the silhouettes may change significantly if the viewpoint changes or 3D objects make non-rigid motions (e.g., articulation). To make things worse, shapes are extracted from 2D images. Heavy noise in shape data is unavoidable due to segmentation errors caused by partial occultation, lighting variation and so on. For the above reasons, many proposed shape descriptors are driven by different aspects of the problem such as robustness to noise or insensitivity to articulation, etc. There are no entirely satisfactory solutions in the shape representation area. A good survey of general shape representation methods can be found in [3, 14]. In this paper, we focus on descriptors requiring contour information only, which are different from descriptors based on the interior of the shape, such as representing each internal point in the interior by a value reflecting the mean time required for a random walk beginning at the point to hit the boundaries [15]. Thus, only some important contour-based shape descriptors are reviewed as follows.

Since shapes are represented by their contours, it is natural to define some simple global shape descriptors, such as area, eccentricity [7], major axis orientation and so on. However, these simple descriptors are coarse representations, and can only discriminate very different shapes. They usually need to be combined with other shape descriptors in order to be more effective. Moment-based [16] and spectral [6, 17] are two more kinds of global descriptors. Moment invariants have been frequently used as some kinds of shape features. In order to reduce the computational burden for moments, Chen [5] presented improved moment invariants which are computed by the shape boundary only, and applied the moment invariants in shape discrimination. Since noise and boundary variations are common in shape data, representing a shape in the spectral domain can alleviate these problems to some extent. Fourier-based shape descriptors [6] and wavelet-based shape descriptors [17] are proposed to transform the shape data into a spectral space, and represent the shape by their coefficients.

Noticing that representing a shape only in a global manner cannot give an entirely satisfactory solution, many recent publications pay great attention to local or hybrid (local/global) descriptors. Shape signature is a well-studied technique, which represents the shape by a one dimension function.

The shape signature corresponds to a descriptive vector in a discrete setting, and is widely used in shape visualization, retrieval, and recognition. Common shape signatures include centroid distance, tangent angle, curvature, chord-length, etc. A high performance signature called contour flexibility is proposed by Xu et al. [9]. Contour flexibility represents the shape by the deformable potential at each landmark on the contour, and copes with the noise and deformation better. However, determining an adaptive bendable size to compute the contour flexibility is a problem. Most of the shape signatures can be usually normalized into being translation and scale invariant, but it is difficult to make them articulation invariant. In general, shape signatures at each landmark are estimated from their local neighbors. It is obvious that representing a shape only by local geometry information will suffer more from noise and local changes.

Common solutions to improve the performance of shape signatures include introducing scale space methods or hierarchical coarse to fine representation strategies to the signatures. Mokhtarian and Mackworth [10] proposed a curvature scale space shape descriptor to overcome the noise and scale problems. In this method, shapes are gradually smoothed by a Gaussian kernel until they become totally convex. The zero-crossings of the curvature function during the smoothing process are located, and form a hierarchical CSS images at last. CSS images can then be used to perform the task of shape matching. However, the matching proves to be very expensive and complex. Other hierarchical descriptions include the shape tree [18], curvature tree [19] etc. Similar to hierarchical descriptors, shape context (SC) [11] captures global and local characterizations of shapes in another kind of hybrid manner, which is receiving more and more attention. For each point on the contour, it is computed by the distributions of the remaining points relative to it. Based on SC, inner distance shape context (IDSC) [12] was proposed to cope with shapes with articulated parts. The authors used the distance of the shortest path inside the shape instead of the traditional Euclidean distance, which achieved better retrieval and recognition performance in the experiments. However, the hierarchical descriptors and the shape context are less compact than shape signatures and computationally demanding for some applications, such as shape matching.

Another way to obtain better descriptors is decomposing contours into different meaningful parts, and building shape descriptors based on this decomposition. By modeling shapes as a combination of approximate convex parts connected by non-convex junctions, Gopalan et al. [20] proposed

articulation-invariant shape descriptors. The performance of their algorithm is directly related to the quality of the shape decomposition. Meanwhile, obtaining a meaningful shape decomposition has been considered as a fundamental problem in many shape-related areas. Convex shape decomposition is the most important kind of decomposition [21, 22]. Based on the observation that electrical charge tends to accumulate at a sharp convexity and vanish at a sharp concavity, Wu and Levine [13, 23] proposed to decompose shapes along the deep concavities which were detected by the electrical charge density distribution (ECDD) on the shapes. However, ECDD cannot be used as an effective shape signature. Firstly, ECDD is not invariant to scale, the charge density is dependent on the resolution. Secondly, ECDD is sensitive to articulation since ECDD is computed by the Euclidean distance metric. Thirdly, due to classic electrical potential, the ECDD method accumulates too much charge at flat locations which does not properly reflect the geometry information of shapes. The experiment result in Table 3 also shows its ineffectiveness in shape recognition. Inspired by the ECDD convex decomposition method, we present the ECDS signature by introducing generalized coulomb potential which represents the part-aware metric and long-range interactions (Section 3.3). ECDS can overcome the above shortcomings of ECDD. Furthermore, although ECDS is a kind of shape signature, it captures both the local geometry information and part structure of the shape in a hybrid manner.

3. Methodology

In this paper, we refer to shape as a single closed contour B of the object O , and B is represented by the separated parameterized landmark sequence $B(n) = \{p_1, p_2, \dots, p_n\}$ in a clockwise direction, where $p_i = (x_i, y_i)$ is the i -th point, with x_i and y_i its corresponding coordinates. To avoid bias, $B(n)$ is uniformly sampled along the contour. The goal of our method is to design a shape signature based on the electrical charge distribution on the shape (ECDS). For the sake of completeness, we first present the ECDS representation and its computation based on the classic ECDD method [23] in Section 3.1 and 3.2, then give the definition of our generalized electrical potential and discuss the characteristics of ECDS.

3.1. The Proposed ECDS Representation

In order to explain the ECDS representation, we begin with three physical facts.

- FACT 1: The electric potential V produced by an isolated point charge Q , at a distance r from the charge, can be expressed by Eq. 1

$$V = \frac{1}{4\pi\epsilon_0} \frac{Q}{r}, \quad (1)$$

where ϵ_0 is the electrical permittivity of space.

- FACT 2: Any charge on an isolated charged conductor will finally reside on the surface and be no longer in motion. The charged conductor then reaches the state of electrical equilibrium.
- FACT 3: Conservation of charge: Charge will be conserved whatever the shape and its corresponding charge distribution is. That is to say, the total amount of charge on the shape remains constant during the process of reaching electrical equilibrium.

Suppose the object O is a charged conductor, and no other charge or conductors exist near it. If a certain amount of charge is placed on O , according to FACT 2, the entire charge will finally reside on the boundary B of O , and B will reach a state of equipotential equilibrium. An observation is that charge tends to accumulate in larger amount at locations of greatest curvature under the electrostatic equilibrium condition. Thus, the charge distribution (CD) on the boundary B captures the geometry information of B , and has larger values in the convex regions and smaller values in concave regions.

Next, we will explain how to compute CD. Since the electrical potential $V(p)$ of the point p on B is contributed to by the entire charge on B , according to Eq. 1, the computation of $V(p)$ can be derived by an integration over B (Eq. 2).

$$V(p) = \frac{1}{4\pi\epsilon_0} \int_B \frac{\rho(p')}{|p - p'|} dB, \quad (2)$$

where $\rho(p')$ is the charge density at position p' of B , $|p - p'|$ is the Euclidean distance between p and p' . Noticing that B has been uniformly parameterized, and represented by the aforementioned landmark sequences

$B(n) = \{p_1, p_2, \dots, p_n\}$, we can discretize the line integral and compute $V(p)$ by Eq. 3

$$V(p) = \frac{1}{4\pi\epsilon_0} \sum_{i=1}^n \frac{Q_i}{|p - p_i|}, \quad (3)$$

where Q_i is the charge on the i -th segment of $B(n)$. The ECDS signature of B can be expressed by $ECDS(B) = [Q_1, Q_2, \dots, Q_n]$ in a discrete version. We will discuss how to compute Q_i in the following section.

3.2. Finite Element Solution

We use Q to represent the total amount of charge on B , which is known beforehand. Thus, according to FACT 3, we have one equality $Q = \sum_{i=1}^n Q_i$. In order to compute Q_i , we need to find more equalities. According to FACT 2, the surface of any charged conductor is an equipotential surface when reaching the state of electrostatic equilibrium. Thus, the electrical potentials at every point p_i of B are with the same value V . That is to say, another n equations are obtained based on Eq. 3. We formulate these equations into a system of linear equations as follows:

$$AX = B. \quad (4)$$

Here

$$X = [Q_1, Q_2, \dots, Q_n, V]^T, B = [0, 0, \dots, 0, Q]^T,$$

and

$$A = \begin{pmatrix} A_{11} & A_{12} & \cdots & A_{1n} & -1 \\ A_{21} & A_{22} & \cdots & A_{2n} & -1 \\ \vdots & \vdots & \ddots & \vdots & \vdots \\ A_{n1} & A_{n2} & \cdots & A_{nn} & -1 \\ 1 & 1 & 1 & 1 & 0 \end{pmatrix},$$

where

$$A_{ik} = \frac{1}{4\pi\epsilon_0} \frac{1}{|p_i - p_k|}. \quad (5)$$

We omit the constant term $\frac{1}{4\pi\epsilon_0}$ in Eq. 5 in practice for computation efficiency, and choose $A_{ii} = 100 * \max_{j \neq i} A_{ij}$ to avoid divisions by zero. The final ECDS representation is obtained by selecting the first n values of the solution X .

3.3. Generalized Electrical Potential

In the above section, we explained how to compute ECDS by the classic model of electrical potential. The ECDS representation reflects the curvature of the shape, and should be more stable to noise since it is computed in a more global manner. However, we find that ECDS is unsatisfactory in some cases, which leads us to discuss its two main drawbacks.

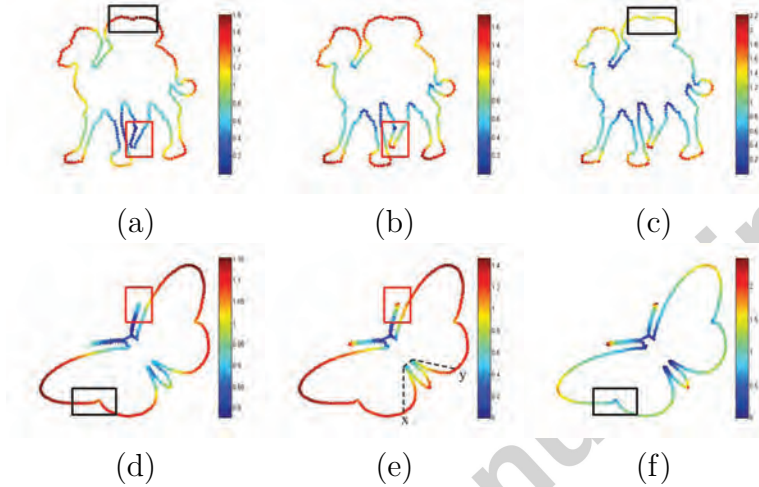


Figure 2: The comparison between classic electrical potential and generalized electrical potential. The first column: ECDS computed by classic electrical potential. The middle column: ECDS computed by introducing inner distance. The right column: ECDS computed by introducing both inner distance and sub-linear exponent $m = 0.2$.

The first drawback is that the classic Euclidean distance in Eq. 5 is not a part-aware metric. If two convex regions are near one another, they should independently accumulate significant charge. However, the reverse is probably true in fact, because charge tends to position itself to increase their distance from one another. Take Fig. 2(a) for example. The feet of the camel ought to accumulate more charge, since they are high curvature regions. However, the foot labeled by the red box disobeys this rule, because this foot is too near the other foot. Introducing the part-aware metric in Eq. 5 can solve this problem. Here, We use the inner distance proposed in [12] instead of the Euclidean distance. The inner distance between two points on a shape contour is defined as the distance of the shortest path connecting them inside the shape. Take Fig. 2(e) for example. The inner distance

between the point x and y is the distance of the path illustrated by the black dotted line. Although the Euclidean distance between the two feet labeled in the red box in Fig. 2(a) is small, the inner distance between them is large. It makes the feet accumulate a larger amount of charge.

The second drawback is that the inverse of the distance used in Eq. 5 decays very fast, making the repulsive force between the far away charge too small and too much charge accumulates at flat locations. Take the first column of Fig. 2 for example, the regions labeled by the black box are flat parts but accumulate significant charge. These labeled parts are slightly further away from the other parts of the shape. Thus, the repulsive forces between them is small, accumulating a significant charge. Introducing a sub-linear exponent m in the norm of Eq. 5 can reduce the decay speed. It penalizes many small discontinuities more than a few large ones and solves this problem to some extent. Take the right column of Fig. 2 for example. The sub-linear exponent $m = 0.2$ performs well to control the repulsive forces between the charge at different distances.

Based on the above two reasons, we finally reformulate Eq. 5 as follows:

$$A_{ik} = \frac{1}{ID(p_i, p_k)^m}, \quad (6)$$

where $ID(p_i, p_k)$ is the inner distance between the point p_i and p_k , $m \in (0, 1)$ is the sub-linear exponent parameter which intuitively controls the influence range. In the limit case $m = 0$, the entire charge has the same influence no matter how far it is. Base on Eq. 6, the calculation formula Eq. 3 for electrical potential can be reformulated as the following Eq. 7. This new kind of potential computed by Eq. 7 is named generalized electrical potential in this paper.

$$V(p) = \frac{1}{4\pi\epsilon_0} \sum_{i=1}^n \frac{Q_i}{ID(p, p_i)^m}. \quad (7)$$

3.4. Characteristics of ECDS

In this section, we will discuss the characteristics and advantages of ECDS. Supposing that a shape S is represented by an uniformly sampled landmark sequence $\{p_1, p_2, \dots, p_n\}$ and $Q = n$ charge is placed on it as mentioned above, $ECDS(S) = [Q_1, Q_2, \dots, Q_n]$ will have some interesting properties and certain advantages over traditional shape descriptors. These properties are summarized as follows.

Invariance: For the given shape S , its ECDS is computed by Eq. 4. Since the element A_{ij} of the coefficient matrix A is a relative measure between the landmark i and j , A is independent of the coordinate system. That is to say, $\text{ECDS}(S)$ is invariant to translation and rotation. And the last equality of Eq. 4 shows $\text{ECDS}(S)$ is invariant to scale. Furthermore, from Eq. 6, A_{ij} is computed by the inner distance between the landmark i and j . An apparent fact is that inner distance is articulation insensitive. Thus, $\text{ECDS}(S)$ is robust to articulation and more effective at capturing structural features of the shape. The scissors in Fig. 3(b) is an articulated form of the one in Fig. 3(a). From the first row of Fig. 3, we see that ECDS of the two scissors are almost the same, showing that ECDS is stable when the scissors make an approximated articulation. The matching comparison in the second row shows that ECDS computed by inner distance is more descriptive than when computed by Euclidean distance.

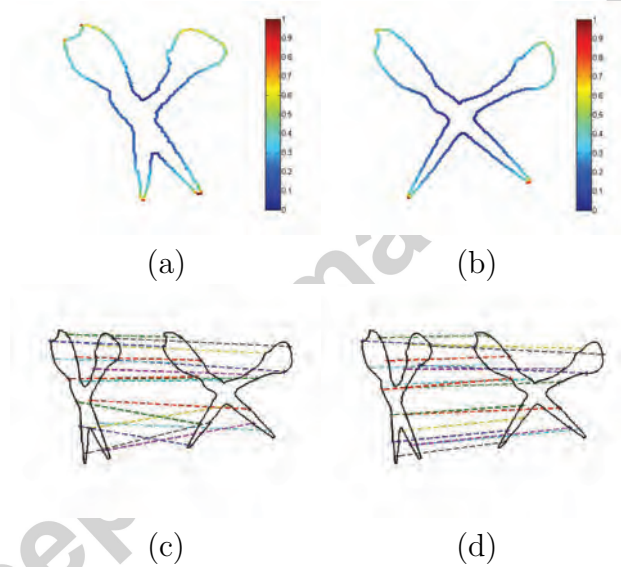


Figure 3: ECDS is insensitive to articulation. The first row: ECDS of a scissor shape (a) and its articulated form (b). The colorbar represents normalized ECDS. The second row: the comparison of matching via ECDS computed by Euclidean distance (c) and via ECDS computed by inner distance (d).

Smoothness and Conservation: $\text{ECDS}(S)$ is derived from the integral function Eq. 2, and approximated by the solution of a system of linear equations Eq. 4. Thus, $\text{ECDS}(S)$ is continuously distributed on the shape S .

Further more, charge cannot be created or destroyed, since n charge has been placed on S , the sum of ECDS is equal to n . It means charge is conserved whatever the shape and its corresponding charge distribution is.

Globality and Locality: A good shape descriptor should capture not only the local geometry information but also the global structure of the shape. The linear equations Eq. 4 consider all the landmarks at once when computing the charge distribution for each landmark. Thus, although the element of ECDS is the local amount of charge for each point, it is determined by all the points on the shape, which is intrinsically different from other shape signatures, such as curvature and contour flexibility. Meanwhile, noticing that these landmarks not contribute equally to the observation position, their contribution is reversely weighted by a sub-linear exponent m of the inner distance between these landmarks and the observation. So, ECDS(S) captures both the local and global information of the shape S , and it is more resistant to noise than curvature-based methods since it is computed in a more global manner according to Eq. 4.

4. Experiments and Performance Analysis

In this section, we evaluate the performance of ECDS via shape matching and retrieval experiments on several public shape databases. The experiments are carried out on a computer with an Intel(R) E5620 2.4GHz CPU and 12GB memory. The code is implemented in MATLAB 2010b with some parts written in C with a MEX interface. Upon obtaining ECDS, dynamic programming (DP) technique is utilized for the following matching procedure. The core code of the DP is provided by Ling and Jacobs [12].

Table 1: The default values of parameters in the experiment

Parameters	ECDS computation			ECDS matching	
	n	Q	m	# starting points k	penalty τ
Value	200	200	0.01	8	0.05

Now we describe the parameters used in the experiments. We uniformly sample $n = 200$ landmark points for each shape, and select the sub-linear exponent $m = 0.01$, the total amount of charge $Q = n$ as the default case. The parameters for computing the inner distance and matching by dynamic programming are chosen according to the suggestion of Ling and Jacobs [12]. The default values of all the parameters in the implementation are listed in

Table 1. In the following section, experiments on different kinds of shape databases will be discussed respectively.

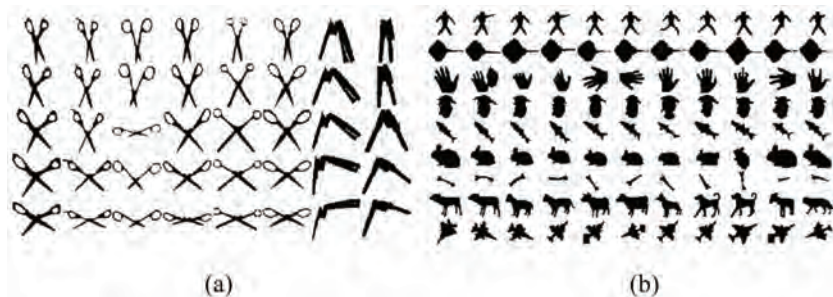


Figure 4: Shapes of two databases. (a) articulation database [12], (b) Kimia database [24].

Table 2: Retrieval results on the articulation database

Method	Rank 1	Rank 2	Rank 3	Rank 4
L_2 (baseline)	25/40	15/40	12/40	10/40
SC [11]	20/40	10/40	11/40	5/40
IDSC [12]	40/40	34/40	35/40	27/40
PWGF [25]	40/40	38/40	33/40	20/40
PWGF + RF	40/40	38/40	36/40	30/40
ECDS (ED)	35/40	24/40	14/40	15/40
ECDS (ID)	40/40	39/40	38/40	31/40

4.1. Experiments on an Articulation Database

In order to evaluate the performance of the ECDS descriptor on shapes with articulations, we perform tests on the articulation data set introduced by Ling and Jacobs [12]. This data set includes shapes with explicit articulations, consisting 8 objects with 5 shapes each, which are shown in Fig. 4(a). For performance evaluation, we exploit the method described in [12]. Each shape is taken as a query for the retrieval test, and the top four similar shapes are selected as ranks 1, 2, 3, 4. The final result is summarized as the number of these shapes falling into the correct category. Noticing there are 40 shapes in the database, so the best result for each rank is 40. Table 2 gives the comparison of ECDS signature with other shape descriptors. Default values are chosen for all parameters in this experiment. Although ECDS is a kind of shape signature which should obtain lower retrieval scores

than shape context based methods such as IDSC, the results show that our method performs best and achieves the highest scores among these methods. It is worthy to point out ECDS performs better than the pairwise geometrical features based method [25] even though their result has been refined.



Figure 5: Example shapes from Part B of the MPEG-7 Core Experiment CE-Shape-1 data set [26].

4.2. Experiments on MPEG7 Shape Database

Part B of the MPEG-7 Core Experiment CE-Shape-1 data set is widely used to test shape matching and retrieval methods. There are 70 groups of objects and 20 binary images in each group. That is to say, the data set contains 1400 shapes. Some example shapes from the set are shown in Fig. 5. Upon obtaining ECDS for the shapes in the database, we match each pair of shapes by their ECDS via a dynamic programming method (DP). The bulleye test is then used to make an evaluation of the matching and retrieval performance. In a Bullseye test, each shape is taken as a query, and the 40 shapes with the smallest distance between the query are retrieved from the database. The Bullseye scores are computed by Eq. 8

$$SCORE = \frac{N}{20}, \quad (8)$$

where N is the number of correct shapes in the 40 retrieval shapes. From Eq. 8, the Bullseye score equals 1 if there are 20 shapes (including the query shape itself) falling into the same group with the query shape in the 40 retrieval shapes. The final Bullseye score is taken as the average of all of the query shapes. The methods with the highest Bullseye score have better performance.

Table 3: Retrieval rate of different methods for the MPEG7 CE-Shape-1 database

Alg.	CSS	SC + TPS	IDSC + DP	PWGF + RF	TAR+DSW	ASC + DP
Score	75.44%	76.51%	85.40%	86.48%	87.23%	88.30%
Alg.	ECDD	KC	LD	CF	ECDS (ID)	ECDS (ED)
Score	67.25%	69.36%	75.28%	82.65%	83.21%	84.31%

Table 3 gives the comparisons between our ECDS descriptor and other descriptors. The shape context methods such as IDSC+DP [12], ASC+DP [27] and the multi-scale descriptor TAR+DSW [19] perform better than shape signatures in general. However, shape context and multi-scale descriptors are less compact and less efficient than shape signatures. For shape signatures (the second row of the table), we compare ECDS with the signatures based on electrical charge density distribution (ECDD), K-curvature(KC), local diameter (LD) and contour flexibility (CF). The classic ECDD has the lowest performance in shape recognition. It is obviously not an effective shape signature. In contrary, ECDS based on Euclidean distance obtains the highest Bullseye scores 84.31 among all of these signatures, and performs better than CF+DP [9], which had previously obtained the highest Bullseye score among shape signatures (to the best of our knowledge). Meanwhile, ECDS compares well with the shape context methods. For the MPEG7 shape database, The recently proposed AIR descriptor [20] obtains the highest retrieval score among all the shape descriptors. However, the AIR descriptor is built based on convex shape decomposition which is a time-consuming process and not a trivial task for complex shapes.

It is interesting to note that ECDS computed by Euclidean distance performs better than ECDS computed by inner distance. It may be because only a few classes of the 70 classes are articulated shapes in MPEG-7 CE-Shape-1. The inner distance ECDS variant has not achieved remarkable results on this test set. Fig. 6 shows class-specific Bullseye scores for ECDS (ED) and ECDS (ID). Comparing to ECDS (ED), ECDS (ID) achieves over 10% percent precision improvement in seven classes which have articulated shapes: the 29th class (device2), the 38th class (elephant), the 45th class (frog), the 49th class (horse), the 60th class (ray), the 61th class (sea snake) and the 65th class (stef).

Performance Analysis of the Parameters: In this part, some parameters in our system are discussed. All the experiments are done on the MPEG7 shape database.

Firstly, the influence of the number of landmarks n is tested. We uni-

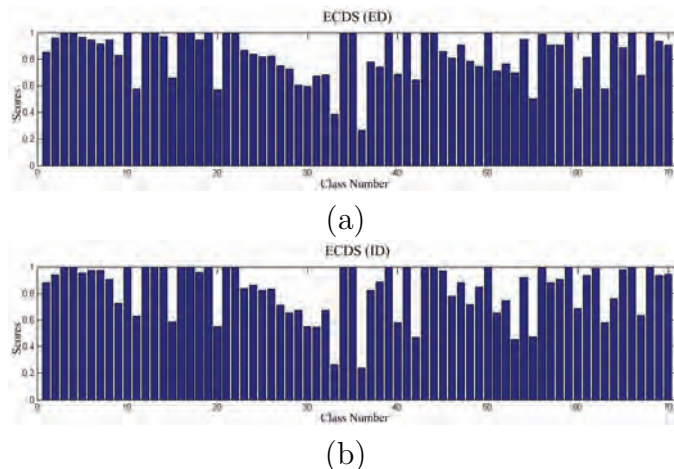


Figure 6: The class-specific Bullseye scores of ECDS computed by Euclidean distance (a) and ECDS computed by inner distance (b).

formly sampled each contour of the MPEG7 shape database by $n = 50$, $n = 100$, $n = 200$, $n = 300$ landmarks and do shape retrieval experiments respectively. The other parameters are chosen in the default case. Fig. 7 (a) illustrates the recognition rate of each case, showing that larger n achieved higher recognition rate. The computation times (descriptor computation per shape + descriptor matching per pair) for ECDS (ID) are listed in Table 4. $n = 200$ is selected for the tradeoff between accuracy and efficiency.

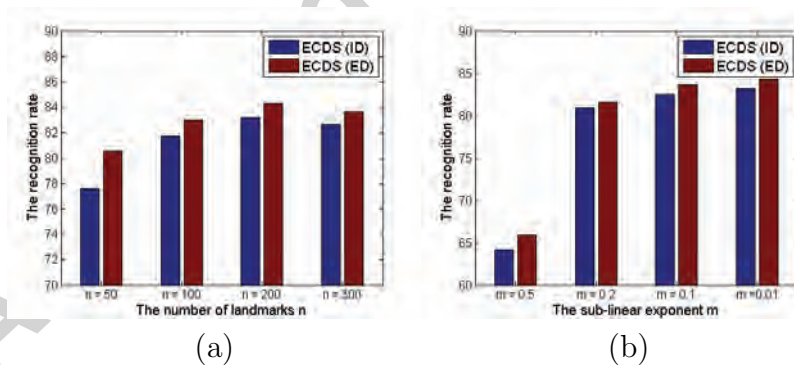


Figure 7: Recognition rate on the MPEG7 shape database with different number of landmarks (a) and different m (b).

Table 4: The comparison of ECDS with different numbers of landmarks

#landmarks	n = 50	n = 100	n = 200	n = 300
ECDS computation	0.03s	0.04s	0.12s	0.31s
ECDS matching	0.3ms	1.0ms	4.3ms	11.8ms

Next, we discuss the parameter sub-linear exponent m . m intuitively controls the repulsive force between the charge. Experiments with $m = 0.5$, $m = 0.2$, $m = 0.1$, $m = 0.01$ are performed. In each case, we select other parameters in the default case. The final recognition rates are shown in Fig. 7 (b). The Bullseye scores is above 80% when $m \leq 0.2$ and smaller m values achieve a higher recognition rate. Thus, $m = 0.01$ is chosen as the default case.

4.3. Experiments on the Kimia Database

Comparisons are done on the shape database provided by Kimia’s group [24]. The data set includes 99 shapes from 9 categories. The shapes are illustrated in Fig. 4(b). In order to evaluate performance, we exploit the method described in [12]. For each retrieval test, the performance is measured according to the correct matching at the top 10 ranks, similarly to the above mentioned articulation database. Obviously, the best result for each rank is 99. We use parameters $n = 300$, $k = 12$, and the other parameters retain their default values. The comparison results are listed in Table 5. Our method compares well with other methods, and obtains the highest score for the first seven ranks.

Table 5: Retrieval results on Kimia 1 data set

Method	1st	2st	3st	4st	5st	6st	7st	8st	9st	10st
SC	97	91	88	85	84	77	75	66	56	37
Gen. Model	99	97	99	98	96	96	94	83	75	48
Shock Edit	99	99	99	98	98	97	96	95	93	82
IDSC+DP	99	99	99	98	98	97	97	98	94	79
PWGF	99	97	98	96	97	97	96	91	83	75
PWGF + RF	99	98	97	99	98	95	97	97	93	78
ECDS(ED)	99	99	99	99	98	98	97	94	91	80

4.4. Experiments on ETH-80 Database

The ETH-80 database [28] contains 80 objects, which are classified into 8 categories: apple, car, cow, cup, dog, horse, pear, tomato. There are 41 images from different viewpoints for each object. Thus, ETH-80 contains

3280 images in total. Some example images are shown in Fig. 8. Note that only the shape contours of the images are used for matching and retrieval. We exploit the standard leave-one-object-out cross-validation testing protocol [12] to evaluate the performance of the existing methods. It means each image is taken as a query, and matched with all the images from the other 79 objects. The candidate with the smallest matching error is returned as the retrieved image. If the retrieved image and the query image fall in the same category, the recognition is considered successful. The final recognition rate is taken as the average of all of the images.



Figure 8: 80 Example images from each object in the ETH-80 database [28].

We test ECDS + DP on this data set with parameter $k = 16$, as in [12]. The other parameters are set to their default values. To the best of our knowledge, the best reported recognition rate on this data set is 93.02%, obtained by the decision tree based approach [28]. This approach is a multi-cue method combining seven single-cue methods. Table 6 lists recognition rate of some single-cue methods. It shows that ECDS achieves the best recognition rate of 89.27% among all of the single cue approaches.

Table 6: The comparison of recognition rates of methods on the ETH-80 database

Method	SC + DP	IDSC + DP	Pairwise GF	ECDS (ID)	ECDS (ED)
Rate	86.40%	88.11%	87.48%	87.84%	89.27%

5. Conclusions

We propose an effective shape signature ECDS by the electrical charge distribution on the shape. ECDS is computed via the solution of a system of linear equations, which makes it continuously distributed and very robust to noise. Furthermore, generalized coulomb potentials representing part-aware metric and long-range interactions are introduced, making ECDS capture the local curvature and the structure information of the shape simultaneously. This makes the signature insensitive to changes in shape articulation. Experiments in shape recognition and retrieval demonstrate that ECDS has some distinguishing characteristics and advantages, such as invariance, conservation and so on. Future works will concentrate on applying ECDS to more shape recognition and classification tasks.

Acknowledgment

This work is supported by NSFC under Grant nos. of 60973115, 60973117, 61173160, 61173162, 61173165, U0935004, 61173103 and 61173102, New Century Excellent Talents in University (NCET-10-0095) of Ministry of Education of China, and this work is also partially supported by Digital signal processing, and the synthesis of an information security system, TR32054, Serbian Ministry of Science and Education. A preliminary version of this paper appeared in the Proceedings of the International Conference on CAD/Graphics 2013 [29].

References

- [1] H. Qi, K. Li, Y. Shen, W. Qu, Object-based image retrieval with kernel on adjacency matrix and local combined features, *ACM Trans. Multimedia Comput. Commun. Appl.* 8 (2012) 54:1–54:18.
- [2] L. d. F. D. Costa, R. M. Cesar, Jr., *Shape Analysis and Classification: Theory and Practice*, 1st ed., CRC Press, Inc., Boca Raton, FL, USA, 2000.
- [3] D. Zhang, G. Lu, Review of shape representation and description techniques, *Pattern Recognition* 37 (2004) 1–19.
- [4] E. R. Davies, *Machine Vision: Theory, Algorithms, Practicalities*, Morgan Kaufmann Publishers Inc., San Francisco, CA, USA, 2004.

- [5] C.-C. Chen, Improved moment invariants for shape discrimination., *Pattern Recognition* 26 (1993) 683–686.
- [6] D. Zhang, G. Lu, A comparative study of fourier descriptors for shape representation and retrieval, in: *Proc. of 5th Asian Conference on Computer Vision*, Springer, 2002, pp. 646–651.
- [7] A. Ion, N. M. Artner, G. Peyré, W. G. Kropatsch, L. D. Cohen, Matching 2d and 3d articulated shapes using the eccentricity transform, *Comput. Vis. Image Underst.* 115 (2011) 817–834.
- [8] R. Gal, A. Shamir, D. Cohen-Or, Pose-oblivious shape signature, *IEEE Transactions on Visualization and Computer Graphics* 13 (2007) 261–271.
- [9] C. Xu, J. Liu, X. Tang, 2d shape matching by contour flexibility, *IEEE Transactions on Pattern Analysis and Machine Intelligence* 31 (2009) 180–186.
- [10] F. Mokhtarian, M. Bober, *Curvature Scale Space Representation: Theory, Applications, and MPEG-7 Standardization*, Kluwer Academic Publishers, Norwell, MA, USA, 2003.
- [11] S. Belongie, J. Malik, J. Puzicha, Shape matching and object recognition using shape contexts, *IEEE Transactions on Pattern Analysis and Machine Intelligence* 24 (2002) 509–522.
- [12] H. Ling, D. Jacobs, Shape classification using the inner-distance, *IEEE Transactions on Pattern Analysis and Machine Intelligence* 29 (2007) 286–299.
- [13] K. Wu, M. Levine, 3d part segmentation using simulated electrical charge distributions, *IEEE Transactions on Pattern Analysis and Machine Intelligence* 19 (1997) 1223–1235.
- [14] S. Loncaric, A survey of shape analysis techniques, *Pattern Recognition* 31 (1998) 983–1001.
- [15] L. Gorelick, M. Galun, E. Sharon, R. Basri, A. Brandt, Shape representation and classification using the poisson equation, *IEEE Trans. Pattern Anal. Mach. Intell.* 28 (2006) 1991–2005.

- [16] G. Papakostas, E. Karakasis, D. Koulouriotis, Novel moment invariants for improved classification performance in computer vision applications, *Pattern Recognition* 43 (2010) 58–68.
- [17] Q. M. Tieng, W. W. Boles, Recognition of 2d object contours using the wavelet transform zero-crossing representation, *IEEE Trans. Pattern Anal. Mach. Intell.* 19 (1997) 910–916.
- [18] P. Felzenszwalb, J. Schwartz, Hierarchical matching of deformable shapes, in: *IEEE Conference on Computer Vision and Pattern Recognition, 2007.*, 2007, pp. 1–8. doi:10.1109/CVPR.2007.383018.
- [19] N. Alajlan, M. Kamel, G. Freeman, Geometry-based image retrieval in binary image databases, *IEEE Transactions on Pattern Analysis and Machine Intelligence* 30 (2008) 1003–1013.
- [20] R. Gopalan, P. Turaga, R. Chellappa, Articulation-invariant representation of non-planar shapes, in: *Proceedings of the 11th European Conference on Computer Vision Conference on Computer Vision: Part III, ECCV'10, Springer-Verlag, Berlin, Heidelberg, 2010*, pp. 286–299.
- [21] H. Liu, W. Liu, L. Latecki, Convex shape decomposition, in: *IEEE Conference on Computer Vision and Pattern Recognition, 2010.*, 2010, pp. 97–104. doi:10.1109/CVPR.2010.5540225.
- [22] Z. Ren, J. Yuan, C. Li, W. Liu, Minimum near-convex decomposition for robust shape representation, in: *IEEE International Conference on Computer Vision, 2011.*, 2011, pp. 303–310. doi:10.1109/ICCV.2011.6126256.
- [23] K. Wu, M. D. Levine, 2d shape segmentation: a new approach, *Pattern Recognition Letters* 17 (1996) 133 – 140.
- [24] T. B. Sebastian, P. N. Klein, B. B. Kimia, Recognition of shapes by editing their shock graphs, *IEEE Trans. Pattern Anal. Mach. Intell.* 26 (2004) 550–571.
- [25] S. Biswas, G. Aggarwal, R. Chellappa, An efficient and robust algorithm for shape indexing and retrieval, *IEEE Transactions on Multimedia* 12 (2010) 372–385.

- [26] L. Latecki, R. Lakamper, T. Eckhardt, Shape descriptors for non-rigid shapes with a single closed contour, in: IEEE Conference on Computer Vision and Pattern Recognition, 2000., volume 1, 2000, pp. 424–429. doi:10.1109/CVPR.2000.855850.
- [27] H. Ling, X. Yang, L. J. Latecki, Balancing deformability and discriminability for shape matching, in: Proceedings of the 11th European Conference on Computer Vision Conference on Computer Vision: Part III, ECCV'10, Springer-Verlag, Berlin, Heidelberg, 2010, pp. 411–424. URL: <http://dl.acm.org/citation.cfm?id=1927006.1927039>.
- [28] B. Leibe, B. Schiele, Analyzing appearance and contour based methods for object categorization, in: IEEE Conference on Computer Vision and Pattern Recognition, 2003., volume 2, 2003, pp. II–409–15. doi:10.1109/CVPR.2003.1211497.
- [29] Z. Li, W. Qu, J. Cao, H. Qi, M. Stojmenovic, Ecds: An effective shape signature using electrical charge distribution on the shape, in: The 13th International Conference on CAD/Graphics, 2013., 2013.